applied sciences

MDPI

Article

Design of U-Shaped Frame of Spaceborne Turntable Based on Multi-Constraint Topology Optimization Method

Jiahao Wang [1,2], Ping Ruan [1,*], Youjin Xie [1], Jingyu Han [1,2], Bo Peng [1,2] and Yun Qu [1]

[1] Key Laboratory of Space Precision Measurement Technology, Xi'an Institute of Optics and Precision Mechanics of CAS, Xi'an 710119, China; wangjiahao2021@opt.ac.cn (J.W.); xieyoujin@opt.ac.cn (Y.X.); hanjingyu@opt.ac.cn (J.H.); pengbo2015@opt.ac.cn (B.P.); quyun@opt.ac.cn (Y.Q.)
[2] School of Optoelectronics, University of Chinese Academy of Sciences, Beijing 100049, China
* Correspondence: ruanp@opt.ac.cn

Abstract: The spaceborne turntable is a piece of precision optical equipment utilized for monitoring space information and facilitating laser communication. The measurement accuracy of optical instruments is correlated to some extent with the mechanical properties of the structure. Addressing the design challenge posed by the U-frame in the spaceborne optoelectronic tracking and pointing turntable, this paper proposes a multi-constraint topology optimization method utilizing Abaqus/CAE and TOSCA. This method offers insights for U-frame design and has undergone scientific validation. Initially, the empirical design structure is established, optimization design areas are defined, and the initial model undergoes pre-processing in Abaqus/CAE. Subsequently, conceptual and mathematical models for topology optimization are developed, with the objective of minimizing structural compliance (thereby maximizing stiffness), and including constraints related to volume fraction, first-order natural frequency, and stress. Utilizing TOSCA, the U-frame topology optimization design is finalized, resulting in an optimized conceptual model. A comparative analysis of the optimized design against the empirical design structure demonstrates a significant 27.53% reduction in maximum stress, enhanced static stiffness, an increase of 11.48% in the first natural frequency, and a 4.3% reduction in mass. Moreover, the turntable that utilizes the optimized design structure not only meets reliability requirements in spacecraft structural design but also provides a stable platform for precise optical load alignment. The static and dynamic performance of the optimized U-frame has been enhanced, effectively mitigating the impact of external excitation on optical instrument measurement accuracy and meeting the lightweight design requirements for the U-frame, thus demonstrating the efficacy of the topology optimization method. This research offers valuable insights into U-frame design for spaceborne optoelectronic tracking and pointing turntables and carries significant guiding implications.

Keywords: precision optical instrument; U-frame of space electro-optical tracking and pointing turntable; finite element analysis; equivalent modeling; multi-constraint topology optimization method; sensitivity calculation; static and dynamic characteristics

check for updates

Citation: Wang, J.; Ruan, P.; Xie, Y.; Han, J.; Peng, B.; Qu, Y. Design of U-Shaped Frame of Spaceborne Turntable Based on Multi-Constraint Topology Optimization Method. *Appl. Sci.* **2024**, *14*, 5842. https://doi.org/10.3390/app14135842

Academic Editor: Muhammad Junaid Munir

Received: 22 March 2024
Revised: 24 June 2024
Accepted: 27 June 2024
Published: 4 July 2024

Copyright: © 2024 by the authors. Licensee MDPI, Basel, Switzerland. This article is an open access article distributed under the terms and conditions of the Creative Commons Attribution (CC BY) license (https://creativecommons.org/licenses/by/4.0/).

1. Introduction

Space-based space object detection constitutes a pivotal technology in Space Situational Awareness (SSA) [1] (pp. 1–3), mitigating the shortcomings of ground-based space detection. The utilization of optoelectronic monitoring equipment on space-based platforms for the detection and collection of space intelligence, as well as for achieving laser communication, is of significant value (Figure 1).

The spaceborne optoelectronic tracking and pointing turntable constitutes a crucial space optoelectronic payload used for maintaining system optical axis stability and executing target acquisition, tracking, and pointing in the space environment in the presence of complex interference factors [2]. This system is widely applied in the realm of space-based

space target detection. Its primary components include azimuth shafting, left and right pitch shafting, support tracking frame, locking mechanism, and carrier stage, to name a few [3] (pp. 203–217). Figure 2 displays the structural diagram of a two-dimensional satellite space turntable system.

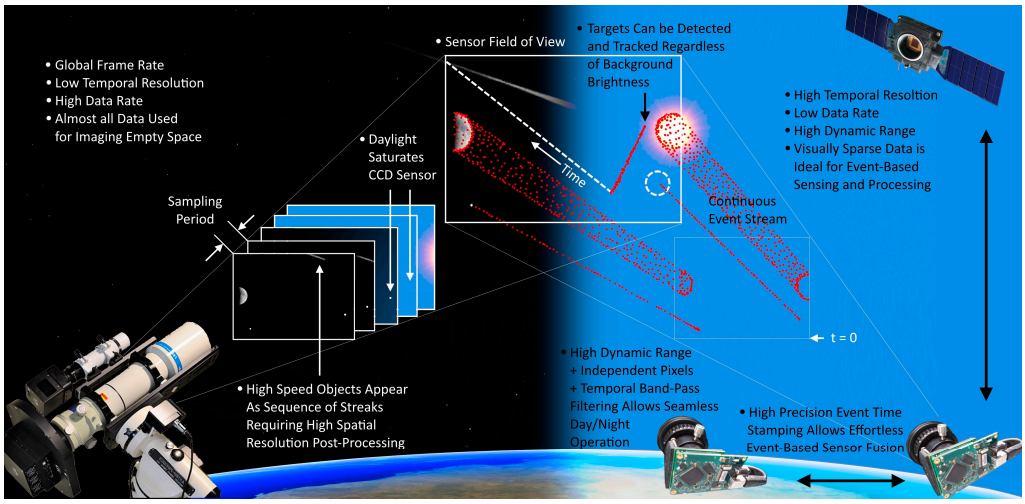


Figure 1. Schematic diagram of Space Situational Awareness.

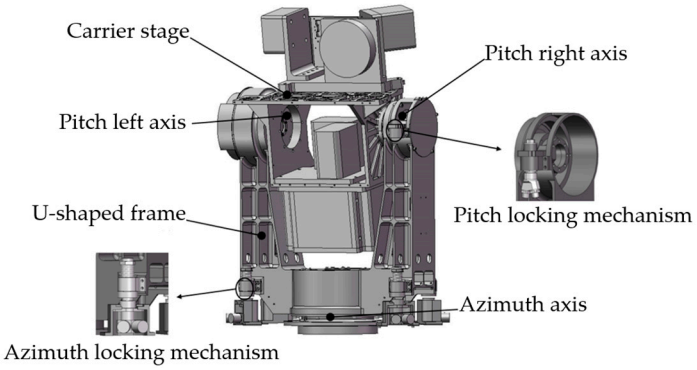


Figure 2. Schematic diagram of the structure of a two-dimensional turntable in a satellite space.

Huang and Zhang summarized the latest progress in space optical instrument design in recent years and pointed out future research directions [4] (pp. 1983–1995). Currently, the design of the spaceborne optoelectronic tracking and pointing turntable's system structure often incorporates a "U"-shaped support tracking frame, attributed to its large structural stiffness, high space utilization rate, and excellent overall performance [5,6] (pp. 879–888). Serving as the primary load-bearing component, the U-frame in the 2-D turntable simultaneously connects both the azimuth and pitch shafting. The photoelectric load is mounted on the carrier platform, interfacing with the pitch shaft system via the pitch shaft hole, and is similarly linked to the azimuth shaft system through the azimuth shaft hole. As a critical component of the spaceborne two-dimensional turntable, the U-frame not only supports the load but also facilitates the transmission of the turntable's attitude motion through its connection to the shaft system and shaft holes. Given the U-frame's considerable mass within the turntable system and the requisite stiffness for its load-bearing capacity, enhancing both its static and dynamic stiffness is crucial to the turntable's performance improvement [7] (pp. 110–115). The structural integrity of spacecraft design is significantly constrained by the launch vehicle's capacity and envelope size, making it a critical parameter. Reducing non-essential loads allows for an increased payload, thereby accommodating more detection tasks and generating greater value. Structure optimization,

pivotal for lightweight design, encompasses size, shape, and topology optimization [8], as depicted in Figure 3.

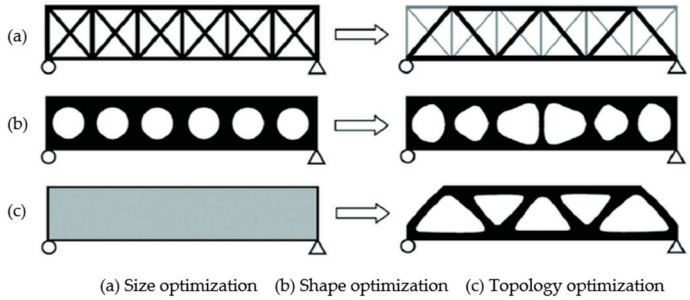


Figure 3. Three ways of structural optimization.

Topology optimization is a key technique in the design of lightweight structures, providing enhanced design flexibility and significant technical advantages, including material reduction and improved structural performance [9]. Owing to advancements in computer technology and finite element theory, its application in engineering projects has progressively increased. Within the aerospace sector, the spaceborne optoelectronic tracking and pointing rotary table is subjected to a complex mechanical environment during launch, characterized by sinusoidal vibration, random vibration, and impacts. This demands that the structure exhibits sufficient dynamic stiffness. Therefore, in light of lightweight design criteria, ensuring the structure's dynamic performance is crucial to prevent performance degradation (e.g., diminished measurement accuracy of optical devices), system or component failures, or damage due to flawed design [10] (pp. 156–162). Kim et al. studied the method of improving the dynamic performance of satellite components through topology optimization and verified its effectiveness [11].

In recent years, many studies have focused on improving topology optimization methods for aerospace structures. Li et al. proposed advanced topology optimization techniques for the design and optimization of aerospace structures [12] (pp. 150–162). Also, extensive research has been conducted on U-frame topology optimization by numerous scholars. For example, Liu Tiejun [5] applied the variable density method for optimizing the topology of a carbon fiber matrix U-frame, with a focus on enhancing structural stiffness. This process resulted in an optimized internal reinforcement layout of the U-frame matrix, leading to a 30% reduction in weight. Modal analysis was subsequently performed to validate the optimization results. Zhang Yongqiang [7] (pp. 110–115) leveraged topology optimization theory, employing the variable density method and the SIMP model, to optimize the topology of a satellite's two-dimensional turntable U-frame. The outcome was a 4.3% weight reduction along with improvements in both dynamic and static mechanical properties. Wang and Chen also obtained similar results when performing structural optimization on satellite support frames, confirming the effectiveness of the optimization method [13] (pp. 975–990). Chen Zhuo [14] utilized the variable density method, integrating the SIMP material interpolation model to maximize structural stiffness, and introduced volume constraints for the topology optimization of a space-based two-dimensional tracking and pointing mechanism's U-frame. This approach facilitated a lightweight structure design, ensuring the turntable system's fundamental frequency met task index requirements and exhibited strong resistance to external interference.

Prior studies have typically prioritized optimizing the static stiffness of the structure, with dynamic performance analysis following optimization. Zhao et al. proposed a multi-constraint optimization method in their study and demonstrated its potential for application in aerospace engineering [15] (pp. 827–844). In contrast, the proposed U-frame topology optimization method by TOSCA integrates dynamic performance analysis directly into the topology optimization process and imposes multiple constraints simultaneously, introducing new ideas and methods for lightweight U-frame structure design.

In this paper, the finite element analysis software Abaqus/CAE and the optimization design tool TOSCA are employed to investigate the topology optimization of the U-frame of a spaceborne optoelectronic tracking and pointing turntable, aiming for a lightweight design without compromising the static and dynamic performance of the structure. The structure of the remaining sections of this paper is outlined as follows:

Section 2 introduces the implementation process of the topology optimization method based on Abaqus/CAE and TOSCA.

Section 3 elaborates on the implementation of the topology optimization method for the U-frame of the spaceborne optoelectronic tracking and pointing turntable.

In Section 4 the post-processing of the U-frame topology optimization results and the performance comparison analysis with the empirically designed structure are conducted.

Section 5 entails the mechanical simulation analysis of the turntable system with the U-frame designed by topology optimization, verifying the effectiveness of the topology optimization method through performance evaluation.

Section 6 concludes the study, summarizing the findings and implications of the research.

2. Topology Optimization Method Based on Abaqus and TOSCA

Several commercial solvers, including TOSCA, OptiStruct, and PERMAS, are available on the market. Table 1 compares the characteristics and performance of these three solvers.

Table 1. Comparison of TOSCA, OptiStruct, and PERMAS solvers.

Feature/Capability	TOSCA	Optistruct	PERMAS
Integration and usability	Integrates with multiple FEA solvers/Medium	Integration with HyperWorks/Easy	Integration with VisPER and ANSA/Hard
Optimization capabilities	Excels in topology optimization and shape optimization	Highly regarded for multi-disciplinary optimization capabilities	High efficiency and capability in handling large-scale problems
Computational efficiency	Depends on the underlying FEA solver	High computational efficiency	High performance and efficiency
Industry applications	Widely used in automotive and aerospace for optimizing structural components	Used across automotive, aerospace, heavy machinery, and consumer goods	Predominantly used in aerospace and automotive sectors

Note: In conclusion, while OptiStruct and PERMAS offer broad optimization capabilities and high computational efficiency, TOSCA distinguishes itself through its flexibility, specialized in topology and shape optimization, and seamless integration with various FEA solvers.

TOSCA, developed by Dassault Systèmes in France, represents an optimization tool widely utilized across diverse fields, including automotive, aerospace, and machinery manufacturing. Specifically, the TOSCA Structure module, grounded in finite element analysis theory, excels at performing efficient topology optimization of structures [16] (pp. 27–31). Owing to its exceptional performance, TOSCA has been integrated as a topology optimization module within Abaqus/CAE, enabling direct access via the Abaqus graphical user interface. This integration facilitates a closed-loop design process, seamlessly integrating structural finite element simulation and topology optimization.

The topology optimization module in Abaqus/CAE provides two types of optimal solution algorithms for selection: condition-based algorithms and sensitivity-based algorithms. The former is typically suited for geometric and contact non-linear problems that are difficult to analyze using sensitivity-based approaches. However, its application is limited by the design response setting. On the other hand, the sensitivity-based algorithm enables the specification of design responses such as structural stiffness, displacement, stress, eigenfrequency, and quality (or volume). This algorithm is adept at addressing a wide range of optimization problems [17]. Considering the design requirements for optimizing the static and dynamic performance of the structure, this study employs a sensitivity-based algorithm for structural topology optimization.

In this paper, we perform topology optimization design of the U-frame for spaceborne optoelectronic tracking and pointing turntables by integrating ABAQUS finite element analysis and TOSCA structural optimization modules. The process initiates with the import of the initial model into Abaqus/CAE and the execution of preprocessing tasks. This entails dividing the optimal design area and non-design area, setting material parameters, establishing static and modal analysis steps, defining load cases and boundary conditions, and executing mesh division. Subsequently, we create a topology optimization task that includes settings for design responses, objective functions, constraints, and geometric constraints. Finally, the job is submitted to acquire the optimization results, thus concluding the entire structural optimization process. The primary process is illustrated in Figure 4.

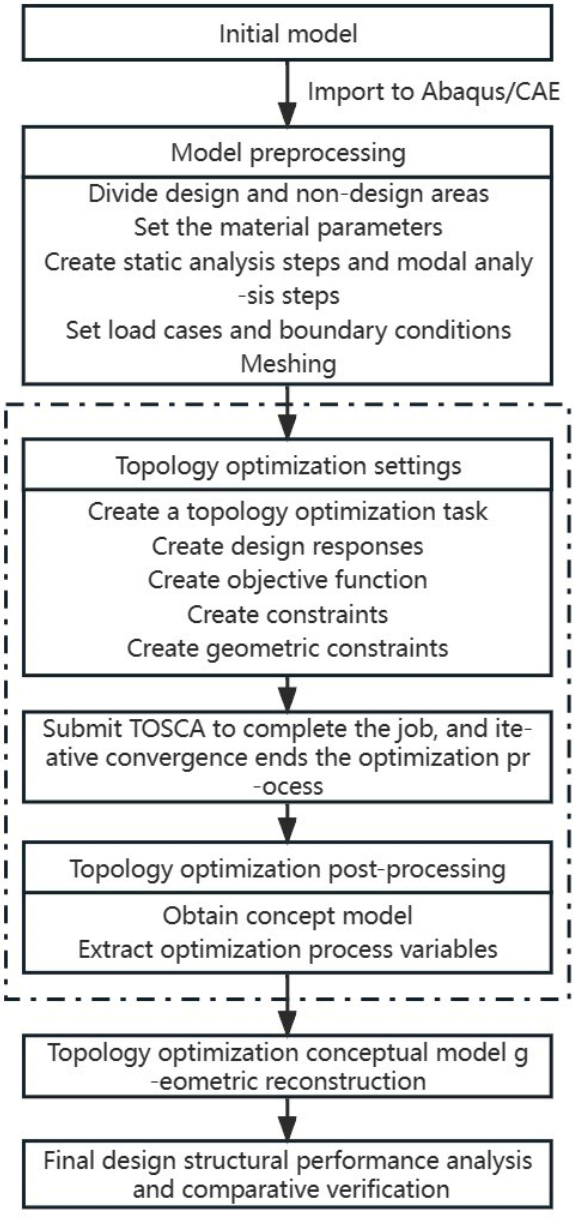


Figure 4. Flow chart of topology optimization based on TOSCA.

3. Topology Optimization Design of U-Frame of Space Electro-Optical Tracking and Pointing Turntable

The U-shaped frame serves a crucial function as a supporting component in the satellite turntable system. The azimuth hole connects to the satellite via the azimuth shaft system and the flange. The bottom cross-arm is firmly secured using an azimuth locking mechanism that employs four explosive bolts. The left and right trunnion holes permit the

passage of the pitch axis system and load-bearing frame, facilitating the accommodation of the photoelectric detection equipment. The pitching movement of the shaft system is limited by the pitch-locking mechanism. However, owing to factors including the substantial load on the turntable, the presence of cantilever installation, and the non-linear connection of the shaft support, the dynamic performance of the turntable system suffers [18]. The U-shaped frame constitutes a critical component within the turntable system, and enhancing its static and dynamic performance is of paramount importance for improving the overall machine performance.

3.1. Subsection Conceptual and Mathematical Models of Topology Optimization

The U-frame structure illustrated in Figure 1 within the turntable system results from empirical design based on weight constraints, with a lack of exploration into the optimal static and dynamic stiffness in the design process. To address this, a conceptual model for the topology optimization of the U-frame is established, taking into account both performance design requirements and lightweight design constraints. Specifically, the optimization objective function aims to minimize the structural compliance of the U-frame (thereby maximizing the overall structural stiffness). Additionally, constraints for multi-constraint topology optimization encompass the volume percentage of the optimized model compared to the initial model, the first natural frequency value of the structure, and the maximum stress value. The mathematical model for topology optimization design is outlined as follows.

The objective function for the topology optimization is to minimize the static strain energy of the U-frame, aiming to maximize the structural stiffness. Multiple constraints are considered in the optimization process, including the percentage of optimized model volume compared to the initial model volume, the first-order natural frequency value of the structure, and the maximum stress value. These constraints enable a comprehensive and multi-constraint topology optimization approach.

The mathematical model for the topology optimization design can be expressed as follows:

$$\mathrm{Min}C = C(\mathbf{x}) = \frac{1}{2}\mathbf{u}^T\mathbf{K}\mathbf{u} \tag{1}$$

$$\mathrm{s.t.}\frac{V(X)}{V_0} \leq \Delta \tag{2}$$

$$\omega \geq \omega_j \tag{3}$$

$$\sigma \leq \sigma_k \tag{4}$$

In these formulas, C(X) represents structural static strain energy and $C(X) = u^T K u$, u is nodal displacement vector, K is structural stiffness matrix, V(X) is topology optimization model volume, V_0 is initial model volume, Δ is volume fraction, ω is structural first-order natural frequency, σ is structural maximum stress, X is design variable, which is expressed as element density, ω_j is the structure first-order natural frequency constraint value, σ_k is the maximum stress constraint value of the structure, $X = \{x_e\}$ is the design variable, $x_e \in [0, 1]\ \forall e = 1, \ldots, N$, represents the cell density, and N is the total number of units.

Equation (1) is the optimization objective function. In the finite element analysis, the change in structural average compliance caused by the change in element density is equal to the change in element strain energy [19] (pp. 239–251), so the problem can be transformed into solving the minimum of structural static strain energy. Formula (2) gives a volume fraction Δ to constrain the volume of the optimized model, so as to realize the constraint on the weight of the model. Formula (3) constrains the first-order natural frequency value of the optimized structure to be greater than or equal to ω_j, and Formula (4) constrains the maximum stress value of the optimized structure to be less than or equal to σ_k.

The fundamental concept in addressing the material distribution problem involves framing it as a challenge of determining the density of each element within the design domain [20]. By employing the SIMP material interpolation model [21] and a gradient-

based optimization solution method, one can derive the objective function in relation to the design variables as detailed below.

$$\frac{\partial C}{\partial x_e} = -px_e^{p-1}\mathbf{u}_e^T\mathbf{K}_e\mathbf{u}_e = -\frac{p}{\chi_e}x_e^p\mathbf{u}_e^T\mathbf{K}_e\mathbf{u}_e = -p\frac{E_e}{\chi_e} \quad (5)$$

where p is the penalty index [21], p = 3 in this study, u_e is the element displacement vector, K_e is the element matrix, and E_e is the element strain energy. It can be seen from Formula (5) that the derivative of the objective function is only related to the element, and since the formula is negative, when the material properties of the element improve (the element density becomes larger), the structural compliance decreases, that is, the stiffness of the structure increases, which is also consistent with the actual physical model.

3.2. The Establishment of the Initial Model

The pitch shaft hole of the U-frame in the spaceborne photoelectric tracking turntable is linked to the pitch shaft system, facilitating the support for the photoelectric detection equipment. The azimuth shaft hole connects to the satellite via the azimuth shaft system and the flange. Five convex platforms are secured with five pyrotechnical bolts to restrict the rotation of the turntable in two directions. Hole features on the side wall were eliminated, while preserving the shape features of the three shaft holes. Finally, the bolt hole was eliminated to finalize the geometric cleaning, yielding the initial model as depicted in Figure 5.

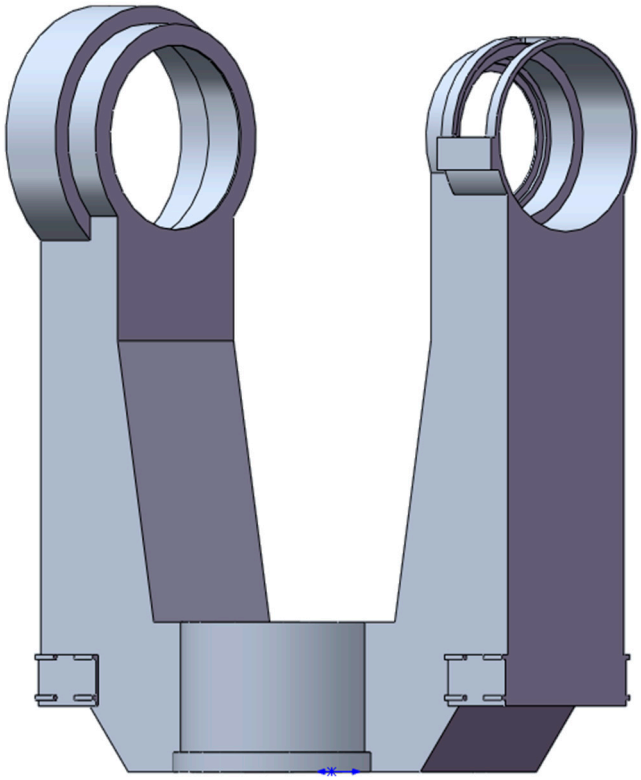


Figure 5. U-frame optimized initial model.

3.2.1. Loading Condition Analysis

The load on the spaceborne optoelectronic tracking and aiming gimbal primarily stems from the optoelectronic detection equipment attached via the pitch axis. Given that the gimbal system experiences a hyper-gravity state during rocket launches, applying multiplied acceleration loads to the gimbal during ground mechanical tests is a standard practice to guarantee the structural reliability of the gimbal. Therefore, with a 70 kg load and 20 g acceleration as conditions, an equivalent load F for the U-shaped frame is determined.

The force is applied at the intersection of the pitch axis hole and the azimuth axis hole, featuring a magnitude of 14,000 N and a direction vertically downward. The simplified mechanical model of the gimbal's U-shaped frame is depicted in Figure 6.

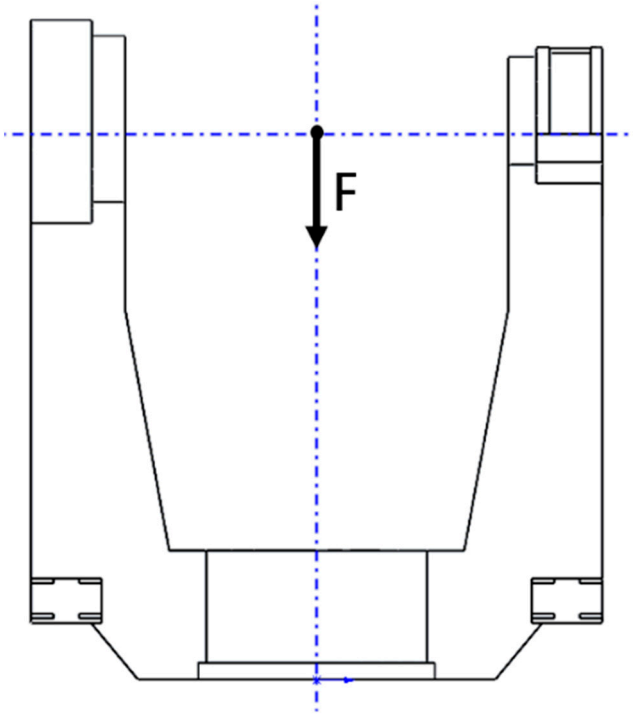


Figure 6. Simplified mechanics model of the turntable U-frame.

3.2.2. Boundary Condition Analysis

The configurations of spaceborne turntables and two-dimensional turntable systems are defined by their connections to the satellite. Connection to the satellite is achieved through the pitch shaft system, flange, and azimuth locking mechanism. Given these conditions, a fixed support constraint is applied at the juncture where the U-shaped frame meets the locking mechanism. This constraint limits movement in all six degrees of freedom.

Additionally, given that the inner wall of the azimuth shaft hole of the U-shaped frame creates a contact pair with the outer surface of the bearing, displacement constraints are applied to the inner wall of the azimuth shaft hole. Axial rotational freedom is permitted, whereas the remaining five degrees of freedom are constrained.

3.3. Model Optimization Pre-Processing

To facilitate the subsequent topology optimization, the model is segmented into two regions: Design–region and Frozen–region. This segmentation aids in selecting the appropriate design regions. The U-shaped frame structure consists of 7075 aluminum alloy, with material parameters as follows: yield strength 455 MPa, Young's modulus 72 GPa, Poisson's ratio 0.33, and density 2810 kg/m^3.

The U-frame is meshed with distinct elements in the non-design area and the optimized design area. For the non-design area, the 10-node tetrahedron element C3D10 is employed, whereas the 8-node hexahedron element C3D8R is utilized in the optimized design area. This meshing method is made to leverage the advantages of both types of elements: hexahedral elements are known for their computational efficiency and accuracy in capturing stress distributions in regular, structured regions, while tetrahedral elements provide flexibility in meshing complex geometries and regions with irregular boundaries. This combination ensures a balance between computational efficiency and the ability to accurately model complex structures, leading to more reliable optimization results. Upon

completion of the meshing process, the U-frame model comprises a total of 168,721 nodes and 111,491 elements. Figure 7 illustrates the grid model of the U-frame.

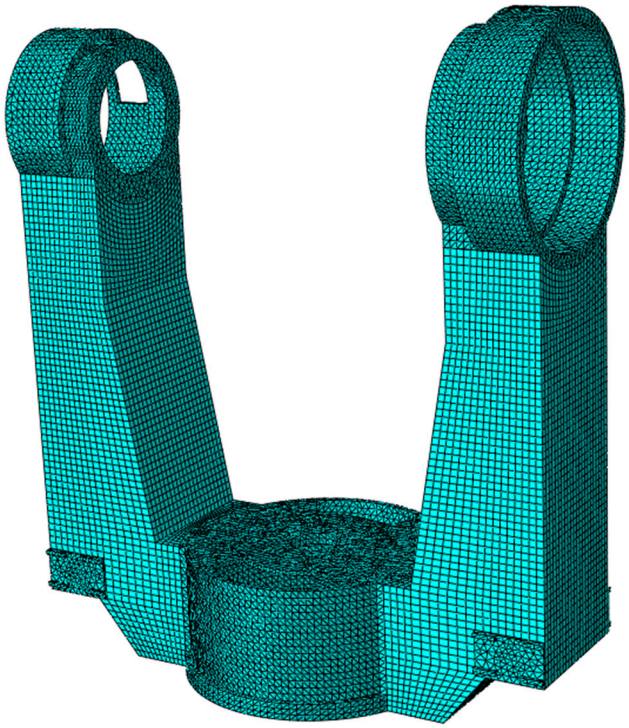


Figure 7. U-frame mesh model.

3.4. Model Geometry Reconstruction after Optimization

Analyzing the U-shaped frame requires establishing both a static analysis step and a modal analysis step, with appropriate loads and boundary conditions applied. In the topology optimization process, an appropriate algorithm is selected, with the objective function and constraint conditions being established. TOSCA is subsequently employed to conduct the topology optimization analysis, yielding a conceptual model as depicted in Figure 8. After 59 iterations, the objective function converges, and the constraint function values meet their limit values. Figure 9 shows the convergence curves of the objective and constraint functions during the topology optimization process.

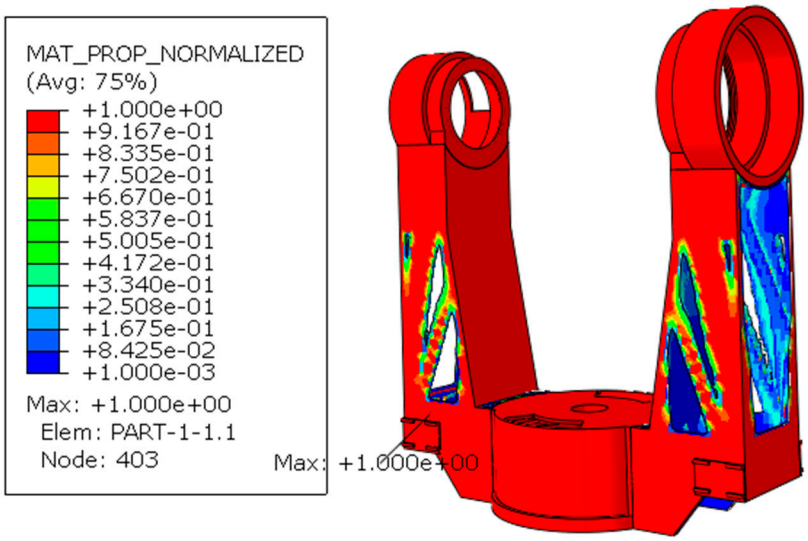


Figure 8. U-frame topology optimization concept model.

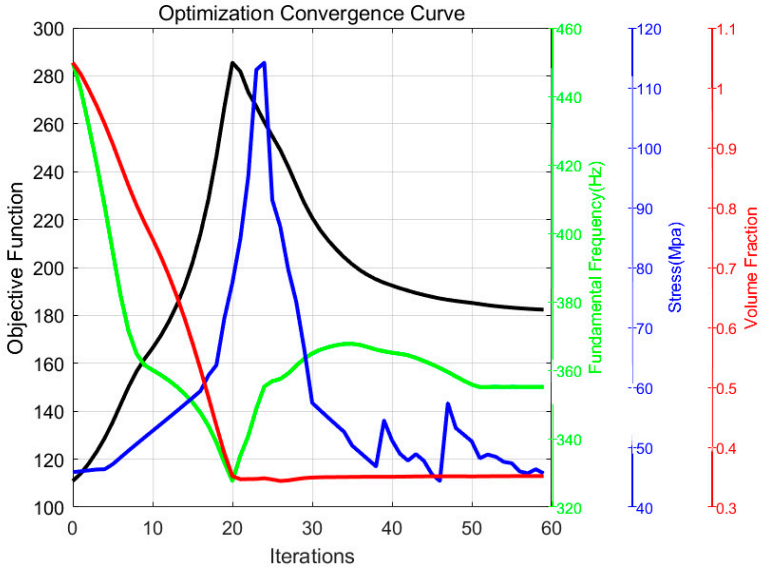


Figure 9. The convergence curves of the objective and constraint functions.

From the optimized conceptual model, material distribution results are derived. Subsequently, unnecessary materials are removed, leading to the creation of the topology optimization conceptual model. This model is then further reconstructed to align with process requirements and manufacturing constraints. Ultimately, the final design structure of the U-shaped frame is obtained, as illustrated in Figure 10b.

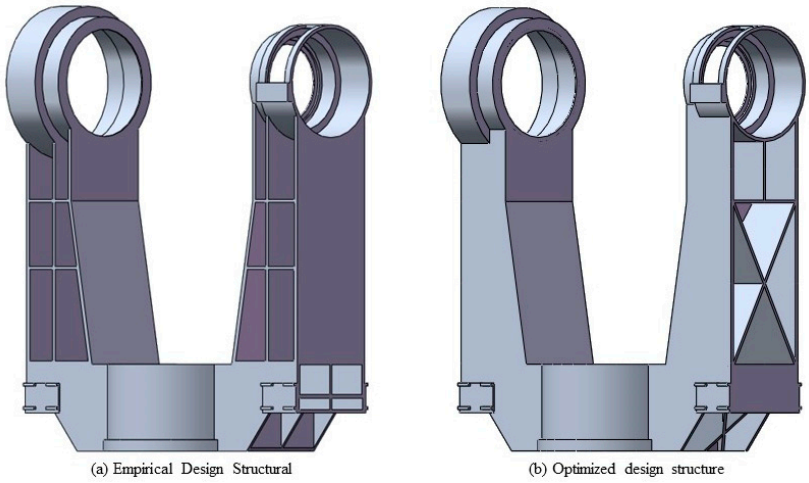


Figure 10. U-shaped frame design structure comparison chart.

As observed from Figure 8, under primarily vertical loads, significant differences emerge between the topology-optimized conceptual model of the U-frame and the empirically designed U-frame structure, particularly in the orientation of side wall holes. This preference for lateral hole placement in the side wall offers valuable insights for engineers in future U-frame design endeavors.

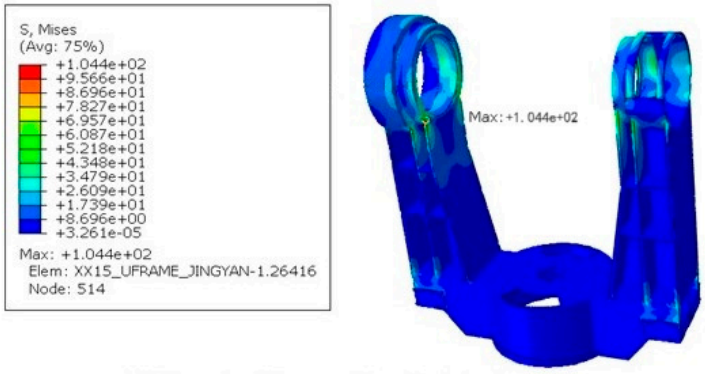
4. Performance Analysis of U-Shaped Frame Optimized Structure

To confirm if the topology-optimized model satisfies the static and dynamic performance design requirements, finite element analysis and a comparison are performed between the empirically designed U-shaped frame structure and the topology-optimized final structure. Static and modal analysis steps are executed for both design structures, as shown in Figure 10a,b, respectively, employing identical load and boundary conditions for performance evaluation and comparative analysis. Mass check is applied

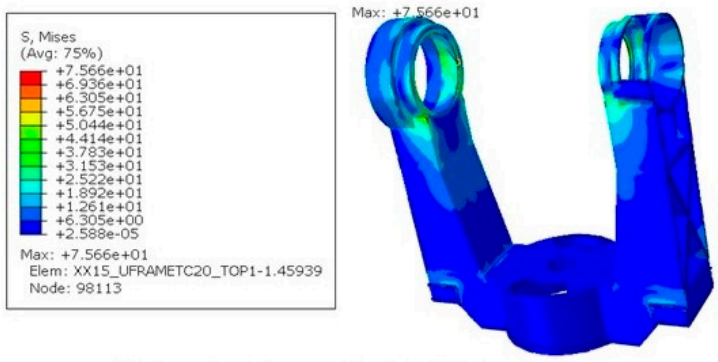
to the topology-optimized final design structure to assess compliance with lightweight design requirements.

4.1. Static Stiffness Check

During the static analysis step, identical loads and boundary conditions are imposed on both the optimized and empirical design structures, leading to a comparison of their maximum stress values. Figure 11 illustrates the stress distribution maps for the optimized and empirical design structures.



(a) Stress cloud diagram of empirical structure



(b) Stress cloud diagram of optimized design structure

Figure 11. Empirical design model and optimization model stress cloud diagram.

Finite element analysis results reveal that under identical working conditions and mesh quality, the empirical design structure's maximum stress value stands at 104.4 MPa, whereas the optimized design structure demonstrates a maximum stress of 75.66 MPa, marking a reduction of 28.74 MPa. This indicates that the U-shaped frame, utilizing the optimized design structure, exhibits enhanced static stiffness.

4.2. Dynamic Stiffness Check

The U-shaped frame, serving as a crucial support component of the gimbal system and comprising a substantial portion of the mass, significantly influences the system's overall dynamic characteristics. Modal analysis reveals that the effective mass attributed to the first five modal frequencies of the U-shaped frame exceeds 90% of its actual mass. Consequently, the first five modal frequencies are extracted from both design structures for a dynamic performance analysis. Finite element analysis results are detailed in Table 2.

Finite element analysis results indicate that although the second-order frequency of the U-shaped frame with the optimized structure experiences a slight decrease, aerospace structures' dynamic performance is predominantly evaluated based on the fundamental frequency. Table 2 demonstrates that, apart from the second-order frequency, there are substantial improvements in the remaining four frequencies, notably in the U-shaped frame's

fundamental frequency, which has risen by 11.48%, thus meeting the structural dynamic performance design requirements. Consequently, the optimized structure demonstrates superior dynamic performance compared to the empirical design structure.

Table 2. Comparison of the first five natural frequencies of the U-shaped frame.

Eigenfrequency	Empirical Design Model	Optimal Design Model	Increase Percentage
mode1	318.37	354.93	11.48%
mode2	364.94	359.12	−1.59%
mode3	430.42	525.85	22.17%
mode4	484.98	538.92	11.12%
mode5	519.98	749.83	44.20%

Note: The dynamic stiffness of a structure is usually measured in terms of first-order natural frequencies.

4.3. Mass Check

The empirical design structure model was subjected to identical geometric modifications as the initial model, encompassing the removal of fillets, bolt holes, and analogous features. Upon assessment, the empirical design structure model's mass was determined to be 5.82 kg. Through topology optimization, the final design structure's mass was reduced to 5.568 kg, resulting in a weight reduction of 4.3%. This optimized U-shaped frame structure design not only meets lightweight design requirements but also simultaneously enhances its static and dynamic performance.

5. Mechanical Simulation Analysis of Turntable System

5.1. Modeling of Spaceborne Optoelectronic Tracking and Sighting Turntable

In practical engineering applications, finite element analysis (FEA) is frequently used to determine the mechanical performance parameters of gimbal systems. Ensuring close alignment of simulation results with actual conditions necessitates the development of a finite element model that precisely mirrors the static and dynamic characteristics of the gimbal. The gimbal's stiffness properties are determined by material attributes, cross-sectional properties of the components, and connection methods among different components. In gimbal systems, modeling non-linear connection parts (e.g., axial connections and locking mechanism connections) through finite element analysis is susceptible to distortion phenomena [3] (pp. 203–217).

Chen Zhuo [14] eliminated pins, bolts, and additional structures during the finite element model simplification of the turntable, utilizing an MPC element to model the locking mechanism's connection and a combination of MPC and spring elements to equivalently represent the bearing part's stiffness. This approach results in exaggerated stiffness at the joint surfaces, deviating significantly from real-world conditions. Feng Yue [22] employed a spring element to model the turntable's bearing connection, deriving axial and radial stiffness coefficients from mechanical test data. While this technique accurately represents the bearing's displacement stiffness, it overlooks the bearing's angular stiffness impact. Despite these modeling approaches achieving an equivalent representation of bearings and locking mechanisms, they fall short in accurately capturing the turntable system's true dynamic characteristics.

This paper employs a generalized spring element to model the shafting and locking mechanism within the rotary table system. The stiffness matrix for the Bushing element at each connection point is derived through theoretical calculations and experimental parameter identification. The motor, harmonic reducer, and other components are removed to simplify the shafting, while firework bolts are eliminated, retaining only the locking supports to finalize the locking mechanism's simplification. Five Bushing elements are established within the azimuth shafting system, the left and right pitch shafting systems, and the locking mechanism, with their stiffness coefficients detailed in Table 3.

Table 3. Five Bushing element stiffness coefficients.

	Stiffness Coefficients					
	K_x **N/mm**	K_y **N/mm**	K_z **N/mm**	K_{θ_x} **N·mm/°**	K_{θ_y} **N·mm/°**	K_{θ_z} **N·mm/°**
Azimuth shafting	2.5×10^5	2.5×10^5	1.1×10^5	2.5×10^7	4.5×10^7	5.5×10^5
Left-pitching shafting	1.6×10^5	1.6×10^5	70,000	5.1×10^7	5.1×10^7	4.0×10^5
Right-pitching shafting	30,000	30,000	300	0	0	0
Pitching locking devices	50,000	50,000	30,000	0	3.0×10^7	3.0×10^7
Azimuth locking devices	15,000	15,000	25,000	0	0	0

Note: The stiffness matrix of the Bushing element at each connection part is obtained by theoretical calculation and experimental parameter identification.

To simplify mesh division and decrease finite element analysis computations, parts of the turntable excluding the shaft system and locking mechanism are streamlined, with features like fillets and holes eliminated. Connecting surfaces between components are rigidly connected. Mass lost through model simplification is compensated by adding 0-dimensional Point Mass. A reinforcement support constraint is applied to the azimuth shaft seat's bottom surface and the locking support, finalizing the turntable's finite element model with 2,029,280 nodes and 1,181,231 grids. Figure 12 displays the meshing model of the turntable.

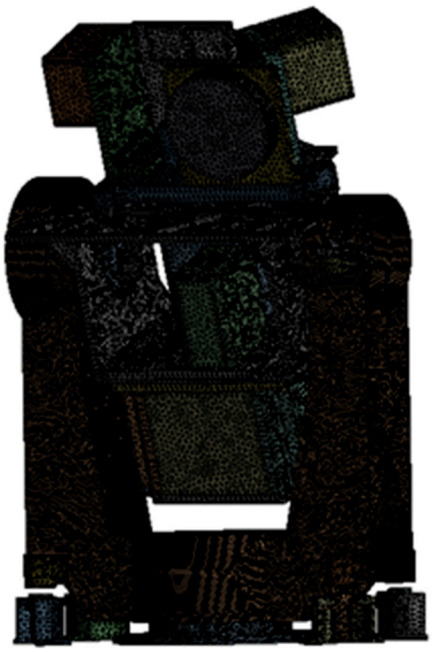


Figure 12. Meshing model of the turntable.

5.2. Static Overload Analysis and Modal Analysis of the Turntable

5.2.1. Static Overload Analysis of Turntable

During the launch, the spaceborne turntable will encounter acceleration loads significantly exceeding gravitational forces, necessitating high structural stiffness to withstand deformation from external loads and prevent structural failure or damage from excessive deformation. Prior to the ground static overload test, the finite element method (FEM) can simulate and assess the structure's maximum stress and displacement, including their locations, serving as a reference for the test and guiding structural strength design. Although the primary acceleration load originates from the vertical direction, additional loads are present in both the X and Y directions. Considering safety margins, engineering experience dictates applying acceleration loads of 4 g in both the X and Y directions and 20 g in the

Z direction to the turntable, allowing for analysis of deformation and stress distribution under various loading conditions. Table 4 displays the stress and displacement cloud maps for the spaceborne turntable under various acceleration loads.

Table 4. Displacement cloud diagram and stress cloud diagram of the turntable under different acceleration loads.

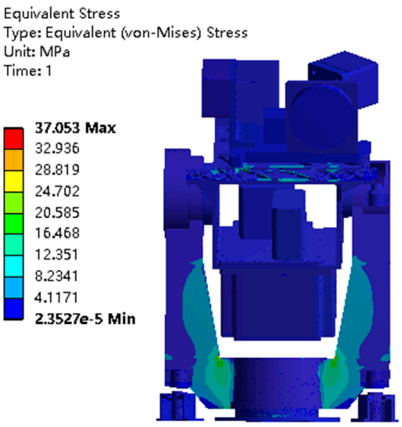
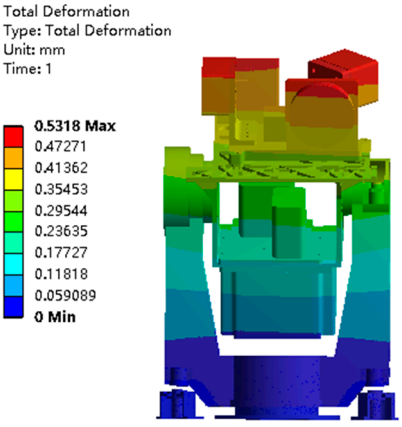
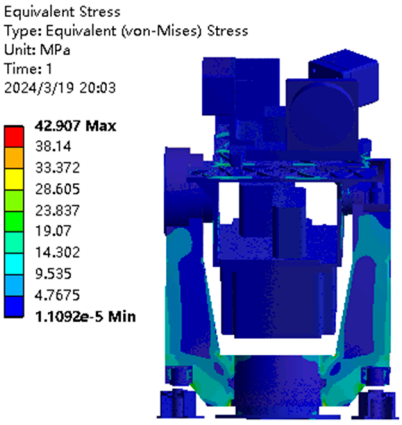
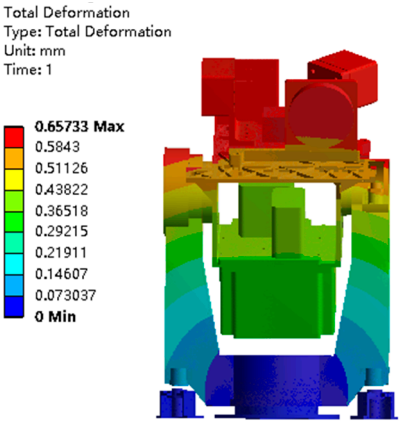
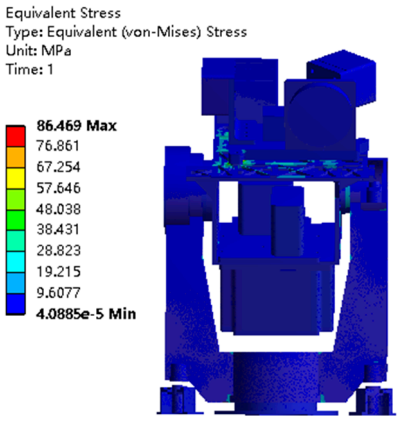
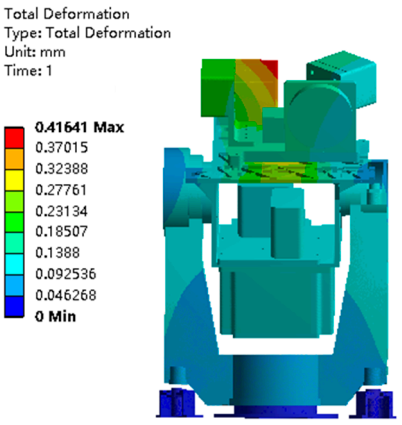
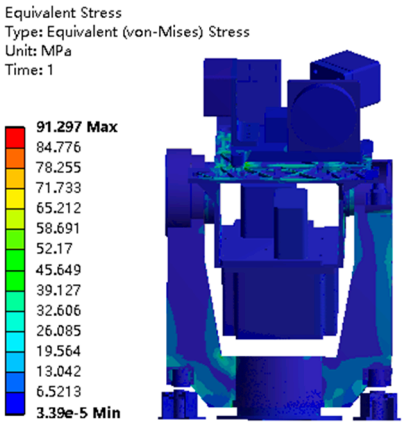
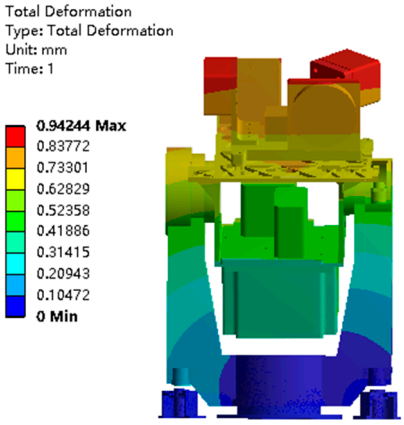
Loading Method	Stress Cloud Diagram	Displacement Cloud Diagram
X_4g		
Y_4g		
Z_20g		

Table 4. *Cont.*

Loading Method	Stress Cloud Diagram	Displacement Cloud Diagram
X_4g, Y_4g, Z_20g		

Note: After performing static overload analysis on the structure, take the maximum stress value of the analysis result as the parameter for strength verification.

The reliability margin for aerospace products is established to offset uncertainties in product design and usage, thereby enhancing product reliability. Spacecraft structural failures do not occur under designed loads, and it is recommended that the safety margin be greater than 0 [23]. The safety margin value (MS) for structural strength design is calculated using the safety factor method, as defined by the following formula:

$$MS = \frac{[\sigma]}{\sigma_{max} \times f} - 1 \quad (6)$$

For the metal material structure, when [σ] is the yield strength of the material, the safety factor f is taken from 1.25 to 1.5 [23]. The yield strength 455 MPa, the maximum stress value 91.297 MPa, and the safety factor 1.5 are replaced into Formula (6), and the safety margin MS value is calculated to be about 2.32, which meets the reliability requirements of spacecraft structure design.

5.2.2. Modal Analysis of Turntable

Modal analysis constitutes the cornerstone of dynamic analysis, enabling the extraction of the model's inherent characteristics, such as frequency and mode shape. This analysis is crucial for selecting parameters pertinent to turntable design, like identifying excitation frequencies and mitigating resonance. Although a continuous elastic body theoretically has an infinite number of natural frequencies, the Block Lanczos method is utilized to solve and analyze the rotary table's first six modes, given that lower-order natural frequencies are more prone to external excitation. Table 5 lists the natural frequency values for the first six orders, and Table 6 showcases the corresponding mode shapes.

The analysis results demonstrate that the overall fundamental frequency of the turntable is 43.2 Hz, exceeding the task index requirement of 40 Hz. This suggests that the turntable is well-equipped to resist external interference, with no risk of structural damage from severe resonance-induced vibration during launch.

Table 5. The first six natural frequency values of the turntable.

Modes	Mode1	Mode2	Mode3	Mode4	Mode5	Mode6
Frequency (Hz)	43.2	45.8	56.3	158.7	164.4	184.2

Note: The primary focus is on the structure's low-order modes. It is essential for the structure's fundamental frequency to exceed the design index.

Table 6. The first six modes of the turntable.

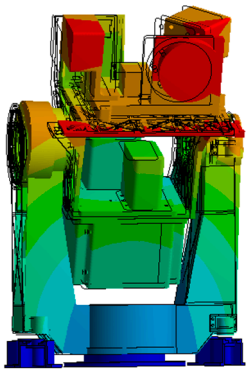
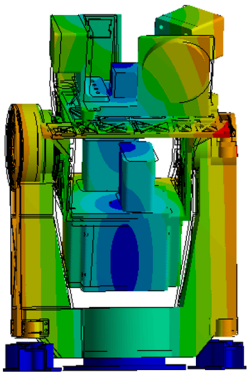
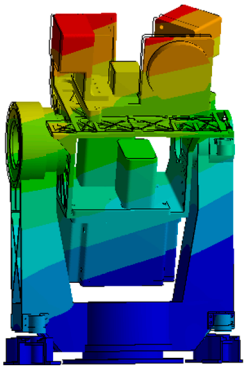
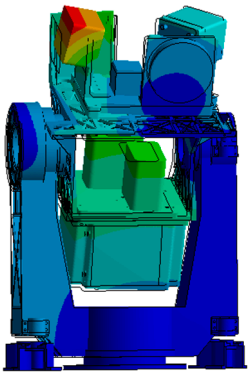
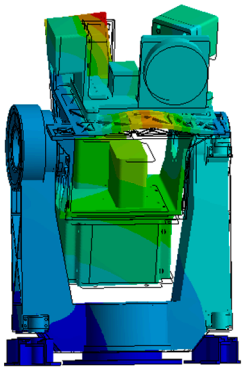
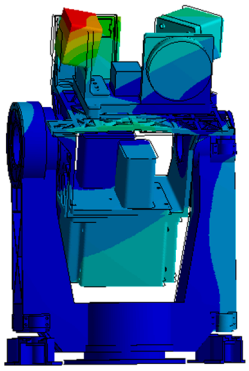
Modes	Mode Diagram	Vibration Form
mode1		Rotate around pitching shafting
mode2		Swing back and forth
mode3		Swing left and right
mode4		Rotate around azimuth shafting

Table 6. *Cont.*

Modes	Mode Diagram	Vibration Form
mode5		Local modal
mode6		Swing up and down

Note: The vibration shapes of the simulation mode and the test mode are basically the same.

6. Conclusions

In this study, utilizing Abaqus/CAE and TOSCA, the topology optimization design of the U-frame structure for spaceborne optoelectronic tracking and sighting turntables is executed. This approach offers a valuable methodology and perspective for the lightweight design of the U-frame structure. The optimization process incorporates both static and dynamic properties of the structure, demonstrating the application of multi-constraint topology optimization in U-frame design.

The performance analysis of the U-frame structure reveals that the optimized structure significantly outperforms the empirical design in terms of mechanical attributes. Specifically, the maximum stress value in the U-frame structure, as determined through topology optimization design, is reduced by 28.74 MPa, while the first natural frequency sees an enhancement of 11.48%. Moreover, when contrasted with the empirical design structure, the optimized version achieves a 4.3% reduction in weight, aligning with lightweight design objectives. Mechanical simulation analysis of the turntable system corroborates that the optimized turntable structure fulfills the reliability standards required for spacecraft structural design, thereby underscoring the efficacy of the topology optimization approach in U-frame structure design enhancements.

The integration of Abaqus/CAE and TOSCA emerges as a potent strategy for optimizing the U-frame structure, attaining a balance between lightweight design and enhanced static and dynamic performances. Additionally, it offers insights into the optimal distribution of holes within the U-frame, guiding future modifications. This study enriches the domain of U-frame structure design for spaceborne optoelectronic tracking and sighting turntables, and suggests new avenues for applying topology optimization techniques to akin engineering challenges.

Author Contributions: Conceptualization, P.R.; methodology, J.W.; software, J.W.; validation, J.W., J.H. and B.P.; formal analysis, Y.Q.; investigation, J.W.; resources, Y.Q.; data curation, J.W.; writing—original draft preparation, J.W.; writing—review and editing, J.W., P.R., Y.X. and B.P.; visualization, J.H. and B.P.; supervision, P.R.; project administration, P.R.; funding acquisition, Y.X. All authors have read and agreed to the published version of the manuscript.

Funding: This research was funded by Member Funding Project of The Youth Innovation Promotion Association CAS, grant number 2022405.

Institutional Review Board Statement: Not applicable.

Informed Consent Statement: Not applicable.

Data Availability Statement: The model and source data used in this article are unavailable due to privacy which protected by industry technology and can be shared as appropriate after stating the ownership institution and purpose via the author's email address.

Conflicts of Interest: The authors declare no conflicts of interest.

References

1. Liu, Y.Z.; Liu, X.B. Research on U.S. Space Situational Awareness Capabilities. *Aerosp. Electron. Countermeas.* **2009**, *25*, 1–3.
2. Cui, K. *Study of the Dynamics Coupling between the Two-Axis Gimbal and the Satellite Bus*; University of Chinese Academy of Sciences: Beijing, China, 2013.
3. Peng, J.L.; Ruan, P.; Xie, Y.J.; Li, Z.G.; Wang, J.H.; Han, J.Y. Analysis of dynamic characteristics of spaceborne photoelectric tracking and aiming turret. *Acta Photonics* **2023**, *52*, 203–217.
4. Huang, Y.; Zhang, M. Recent Advances in Spaceborne Optical Instruments Design. *Opt. Precis. Eng.* **2022**, *30*, 1983–1995.
5. Liu, T.J. *Lightweight Structure Design and Analysis of High-Precision Space Two-Dimensional Turntable*; Changchun University of Technology: Changchun, China, 2013.
6. Wang, W.B.; Wang, T.F.; Guo, J. Analysis of spaceborne photoelectric capture tracking and aiming control technology. *China Opt.* **2014**, *7*, 879–888.
7. Zhang, Y.Q.; Liu, Z.H.; Li, Z.G.; Xie, Y.J. Structural optimization design of the space two-dimensional turntable collimator. *Infrared Laser Eng.* **2017**, *46*, 110–115.
8. Zuo, K.T. *Research on the Theory and Application of Topology Optimization of Continuum Structures*; Huazhong University of Science and Technology: Wuhan, China, 2004.
9. Sun, S.P. *Research on Key Theories and Methods of Topology Optimization of Materials and Structures*; Northwestern Polytechnical University: Xi'an, China, 2008.
10. Gu, S.N.; Xu, B.; Rong, J.H.; Jiang, J.S. New progress in structural dynamics design optimization methods. *Mech. Strength* **2005**, *27*, 156–162.
11. Kim, J.; Lee, S.; Park, M. Enhancing Dynamic Performance of Satellite Components through Topology Optimization. *Int. J. Mech. Sci.* **2022**, *215*, 106837.
12. Li, X.; Zhang, Y.; Wang, H. Advanced Topology Optimization Techniques for Aerospace Structures. *J. Aerosp. Eng.* **2023**, *30*, 150–162.
13. Wang, Z.; Chen, J. Structural Optimization of Satellite Support Frames. *Struct. Multidiscip. Optim.* **2023**, *68*, 975–990.
14. Chen, Z. *Structural Design and Analysis for Mechanical and Thermal Property of a Spatial-Based Two-Dimensional Tracking and Pointing Mechanism*; University of Chinese Academy of Sciences: Beijing, China, 2015.
15. Zhao, L.; Liu, Q.; Chen, X. Multi-Constraint Optimization Methods in Aerospace Engineering. *Eng. Optim.* **2023**, *55*, 827–844.
16. Zhang, N.; Zhao, X.Y.; Zhang, D.W.; Shi, Y.G. Topology optimization method of precision horizontal machining center slide plate based on TOSCA software. *Mech. Des.* **2017**, *34*, 27–31.
17. Zhang, N. *Topology Optimization Method for Key Large Parts of Precision Horizontal Machining Center Based on TOSCA*; Tianjin University: Tianjin, China, 2017.
18. Yan, Z.X. *Design and Analysis of Space-Borne Two-Dimensional Tracking Turntable Resistant to Space Environment*; Graduate School of Chinese Academy of Sciences; Shanghai Institute of Technical Physics: Shanghai, China, 2015.
19. Chu, D.N.; Xie, Y.M.; Hira, A.; Steven, G.P. Evolutionary structural optimization for problems with stiffness constraints. *Finite Elem. Anal. Des.* **1996**, *21*, 239–251. [CrossRef]
20. Guo, D.Z. *Efficient Architecture and Software Development for Three-Dimensional Static/Dynamic Topology Optimization Based on Variable Density Method*; Hunan University: Changsha, China, 2021.
21. Bendsøe, M.P.; Sigmund, O. *Topology Optimization*; Springer: Berlin/Heidelberg, Germany, 2004.

22. Feng, Y. *Dynamic Analysis and Experimental Research on Two-Axis Turntable in Space*; Harbin Institute of Technology: Harbin, China, 2011.
23. *GB/T 40537-2021*; Aerospace Product Margin Design Guide. National Aerospace Technology and Application Standardization Technical Committee (SAT/TC 425): Beijing, China, 2021.

Disclaimer/Publisher's Note: The statements, opinions and data contained in all publications are solely those of the individual author(s) and contributor(s) and not of MDPI and/or the editor(s). MDPI and/or the editor(s) disclaim responsibility for any injury to people or property resulting from any ideas, methods, instructions or products referred to in the content.